Thermal- and Piezo-Tunable Flexural-Mode Resonator with Piezoelectric Actuation and Sensing

Citation for published version:
Svilii, B, Wood, G, Mastropaolo, E & Cheung, R 2017, 'Thermal- and Piezo-Tunable Flexural-Mode Resonator with Piezoelectric Actuation and Sensing', *Journal of Microelectromechanical Systems*, vol. 26, no. 3, pp. 609-615. https://doi.org/10.1109/JMEMS.2017.2680465

Digital Object Identifier (DOI):
10.1109/JMEMS.2017.2680465

Link:
Link to publication record in Edinburgh Research Explorer

Document Version:
Peer reviewed version

Published In:
Journal of Microelectromechanical Systems

Thermal- and Piezo-Tunable Flexural-Mode Resonator with Piezoelectric Actuation and Sensing

B. Sviličić, G. S. Wood, *Member, IEEE*, E. Mastropaolo, *Member, IEEE*, and R. Cheung, *Senior Member, IEEE*

***Abstract*—This paper reports on a piezoelectrically actuated and sensed flexural-mode microelectromechanical (MEMS) resonant device with electrothermally and piezoelectrically tunable resonant frequency. The device is designed as a multilayer circular membrane (diaphragm) resonator with a lead-zirconium-titanate piezoelectric actuator and sensor as well as platinum electrothermal tuning electrodes placed on the top of a silicon-carbide diaphragm. The design enables active electrothermal frequency tuning independent of the piezoelectric input/output operation of the device. The performance of the fabricated device has been tested using two-port transmission frequency response measurements that are performed at atmospheric conditions. Electrothermal tuning and piezoelectric tuning introduce the unique feature of shifting the resonant frequency downward and upward, respectively. The resonant frequency has been tuned by applying DC voltages in the range 0 V – 5 V. The measurements have shown that an 886 kHz device exhibits a frequency tuning range of about –8,400 ppm when tuned electrothermally, and a tuning range of about +2,400 ppm when tuned piezoelectrically. Simulated results have shown that the wider frequency range for electrothermal tuning is a result of larger change in induced stress in the diaphragm for a given DC voltage, as well as the fact that the electrothermal tuning mechanism effectively serves to relax the residual tensile stress in the diaphragm.**

***Index Terms*—MEMS, resonator, tunable filter, piezoelectric actuation, piezoelectric sensing, electrothermal tuning, piezoelectric tuning.**

I. Introduction

MICROELECTROMECHANICAL SYSTEMS (MEMS) resonators have been used in wide range of applications, such as oscillators [1], [2], filters [2], gyroscopes [3], accelerometers [4], and sensors [5]. One of the main problems affecting MEMS resonators consists of resonant frequency shifts arising from changes in the ambient conditions (variations of temperature and pressure) or fabrication process uncertainties (variations of geometrical dimensions and material properties, residual stress) [6]. Therefore, capability of active frequency tuning that is repeatable and reversible is a vital feature for MEMS resonators to work effectively on a specific frequency [7].

Manuscript received July 7, 2016. The work of B. Sviličić was supported in part by the Croatian Science Foundation and University of Rijeka.

B. Sviličić was with the Scottish Microelectronics Centre, Institute for Integrated Micro and Nano Systems, School of Engineering, The University of Edinburgh, Alexander Crum Brown Road, Edinburgh EH9 3FF, United Kingdom. He is now with the Faculty of Maritime Studies Rijeka, University of Rijeka, Studentska ulica 2, 51000 Rijeka, Croatia (e-mail: svilicic@pfri.hr).

E. Mastropaolo, G. S. Wood, and R. Cheung are with the Scottish Microelectronics Centre, Institute for Integrated Micro and Nano Systems, School of Engineering, The University of Edinburgh, Alexander Crum Brown Road, Edinburgh EH9 3FF, United Kingdom.

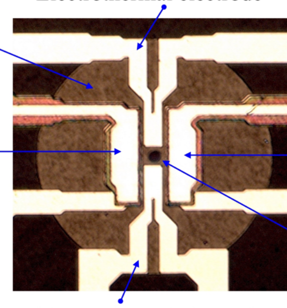

Fig. 1. Optical micrograph of a fabricated device with the piezoelectric input and output ports and with the electrothermal tuning electrodes placed on the top of the diaphragm with a central hole.

Piezoelectric and electrostatic transductions are leading techniques for electrical induction and detection of mechanical vibrations in MEMS resonators. The advantages of piezoelectric transduction over the electrostatic transduction include stronger electromechanical coupling, lower impedance and lack of the need for any DC voltage for the operation [8]. In addition, the fabrication process of piezoelectric resonators is relatively simpler as the electrostatic transduction requires stringent nanometric control of the electrode-to-resonator gap spacing. However, one of the major drawbacks of piezoelectric resonators is the need of active frequency tunability to maintain performance. The reported active frequency tuning solutions for piezoelectric MEMS resonators include the fine-tuning induced piezoelectrically [9], [10], electrostatically with integrated capacitive structure [11]-[13], and electrically via feedback-based tuning technique [14] and by using phase change material programmable vias [15].

On the other hand, the use of electrothermal transduction for performing tuning has been attracting increasing attention as a means of allowing simple design and fabrication process. Electrothermal tuning has been integrated together with a variety of actuation techniques (electrostatic [16]-[19], electrothermal [20], [21] and magnetomotive [22]) showing the possibility of achieving wide tuning range with low DC voltages. In addition, electrothermal transduction has been used for introducing localized heating on contour-mode aluminium nitride (AlN) film bulk resonators in order to fine-tuning the operating frequency of the devices [23]-[25].

This paper reports on the design, testing and simulation of a piezoelectrically transduced flexural-mode MEMS resonator with electrothermally and piezoelectrically tunable resonant frequency (Fig. 1). The device is designed as a multilayer structure with two piezoelectric ports placed on top of the resonant layer made of cubic silicon-carbide (3C-SiC). Additional top electrodes are integrated to perform electrothermal tuning independently of the piezoelectric transduction. The design and position of the piezoelectric ports and electrothermal electrodes are optimized to achieve effective piezoelectric transduction and electrothermal tuning respectively. The performance of the fabricated device has been tested by performing two-port transmission frequency response measurements in atmospheric conditions. In addition, finite element method (FEM) simulations have been performed in order to relate the resonant frequency tuning of the resonator to the piezoelectrically or electrothermally induced stress in the multilayer structure.

II. Theory

A. Piezoelectric actuation and sensing

The piezoelectric effect refers to the ability of a material to deform mechanically when applying an electric field. In addition, the piezoelectric effect is associated with the reverse process, where the electrical polarization of a material is altered as a result of a mechanically induced deformation. The structure of the fabricated device consists of a piezoelectric material layer deposited on the top of the resonant structure allowing for piezoelectric actuation and sensing.

If a voltage is applied across the material, creating an electric field, E_3, then the induced stress, σ_x, is given by [26]

$$\sigma_x = \frac{\varepsilon_x - d_{31}^{eff} E_3}{s_{11}^{eff}} \tag{1}$$

where ε_x is the strain, s^{eff}_{11} is the effective elastic compliance and d^{eff}_{31} is the effective piezoelectric coefficient. The strain, ε_x, can be expressed as

$$\varepsilon_x = \left(s_{11}^{E} + d_{311}E_3\right)\sigma_x + \left(d_{31} + m_{31}E_3\right)E_3 \tag{2}$$

where s^{E}_{11} the elastic compliance, d_{311} is the electroelastic compliance coefficient, d_{31} is the piezoelectric strain coefficient and m_{31} is the electrostrictive compliance coefficient.

Applying an AC voltage will result in an alternating compression and expansion of the piezoelectric layer, which will actuate the entire multilayer structure. For sensing, the mechanical oscillations of the resonator can be detected by measuring the induced alternating voltage, which will match the oscillation frequency of the structure.

B. Electrothermal and piezoelectric tuning

The resonant frequency of a structure can be modified by including built-in stress in the device, as will be discussed later, and by inducing additional stress [21]. If a DC voltage is applied across an electrode that is positioned on top, then the temperature increase, ΔT, is proportional to the power dissipated per unit volume. The power dissipation will result in electrothermal heating of the resonator. A material will expand by a change in length, δ_L, as given by

$$\delta_L = \alpha L \Delta T \tag{3}$$

where α in the thermal expansion coefficient (TEC) and L is the initial length. As a result of the fixed anchors of the resonator, the thermally-induced expansion of the material is impeded, which results in a thermal stress, σ_T, given by

$$\sigma_T = \frac{\delta_L E}{L} \tag{4}$$

If (4) and (5) are combined, the thermal stress can be expressed in terms of the change of temperature, as follows

$$\sigma_T = \alpha E \Delta T \tag{5}$$

It can be seen that the thermal stress will be increased when the temperature of the structure increases as a result of the Joule heat induced by the DC voltage applied to the electrode [21].

In addition to electrothermal tuning, the resonant frequency can be tuned by applying a DC voltage to the piezoelectric material on top of the diaphragm. As has been shown in (1), a stress proportional to the electric field will be induced in the piezoelectric layer.

III. Device Design and Operation Principle

The device is designed as a multilayer circular membrane (diaphragm) resonator. In this work, 3C-SiC as been used as structural material due to its excellent mechanical properties and robustness compared to other materials such as silicon nitride or oxide [27]-[29]. The high value of Young's modulus and the relatively low mass density allow 3C-SiC structures to resonate at higher frequencies than Si structures of identical dimensions. The use of 3C-SiC as structural material contributes towards the stability of the resonant frequency in critical environmental conditions (i.e., temperature higher than room temperature). The piezoelectric actuator (input port) and sensor (output port) formed of lead-zirconium-titanate (PZT) sandwiched between two platinum (Pt) electrodes are placed on the top of the 3C-SiC layer forming vertical flexural-mode resonator. The piezoelectric ports are placed close to the central hole of the diaphragm in order to maximize vibration amplitude and, on the sensing side, to achieve a high electrical output. In addition, effective piezoelectric ports area covering the diaphragm's surface from the hole to the edge is reduced to increase the quality (Q) factor [30], [31]. When applying an AC signal to the input port, the PZT layer induces a time-varying bending moment that excites the structure into vibration. The resulting vertical vibration is experienced as a strain in the PZT layer of the output port and an alternating voltage with a frequency equal to the mechanical vibration frequency can be detected. The use of PZT, due to its high piezoelectric coefficient, offers enhanced electromechanical coupling [8].

In order to combine the advantages of the piezoelectric transduction with the electrothermal tuning method, heating electrodes made of Pt have been designed on the top of the 3C-SiC diaphragm. The two-layer structure consisting of two different thermal expansion coefficient materials allows an enhanced electrothermally induced mechanical strain [32]. The configuration of two electrodes positioned close to the central hole was chosen to maximize the induced temperature and heated area [33]. As the thin Pt layer electrodes cover a small part of the diaphragm surface, they do not significantly reduce the piezoelectric sensitivity of the fundamental resonant frequency.

IV. Experimental Details

A. Fabrication

The device is fabricated with diaphragm radius of 150 µm and central hole radius of 10 µm. In [34], we have presented the detailed fabrication process of piezoelectrically transduced 3C-SiC diaphragm resonators. The fabrication process consists of three major phases: (i) growth of a 2 µm thick 3C-SiC layer on Si followed by the deposition of a Pt/PZT/Pt layer with thicknesses of 100/500/100 nm; (ii) patterning of the piezoelectric ports and electrothermal electrodes by processing Pt and PZT layers; (iii) patterning of the circular hole in the 3C-SiC layer and release of the Si sacrificial layer. The fabrication process flow together with the layers thicknesses and the diaphragm with a central hole dimensions are shown in Fig. 2.

B. Measurement setup

The fabricated device testing has been carried out using an HP 8753C network analyzer in the two-port measurement configuration. The device has been tested in an RF probe station and directly connected with ground-signal-ground probes to the network analyzer, without use of any interface electronic circuitry between the device and the network analyzer. The transmission frequency response measurements have been performed after calibrating the network analyzer (two-port short-open-load-through method) and under atmospheric condition and at room temperature. The resonant frequency tuning has been performed with an external stabilized DC power supply.

C. Simulations

In order to explain the resonant frequency tuning behavior of the devices, FEM simulations have been performed with *CoventorWare*. A meshed model of the final structure depicted in Fig. 2 has been created and used for simulation. The mechanical response of the fabricated device under the influence of the applied electrothermal and piezoelectric tuning DC voltages has been investigated with the induced stress in the 3C-SiC layer being extracted from the simulation results.

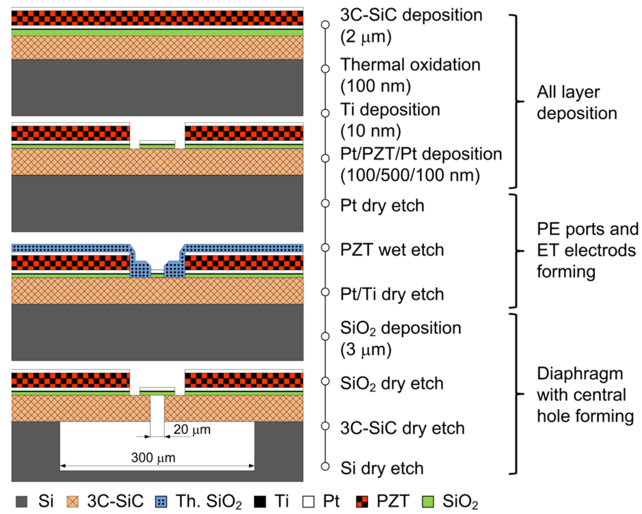

Fig. 2. Fabrication process flow and physical dimensions of the fabricated device.

V. Results and Discussion

A. Electrothermal tuning

Fig. 3 shows transmission magnitude plots of the device that was piezoelectrically actuated and electrothermally tuned. A resonant frequency (untuned resonant frequency) of 886 kHz has been measured using an input AC signal power of 10 dBm provided by the network analyzer and with no DC voltage applied. Quality factor of 205 has been calculated by taking the ratio of the resonant frequency and the 3-dB bandwidth of the device. The resonant frequency has been tuned electrothermally by simultaneously applying DC voltages to both electrothermal electrodes (see the inset of the Fig. 3). As the DC voltage is increased from 0 V to 5 V, a resonant

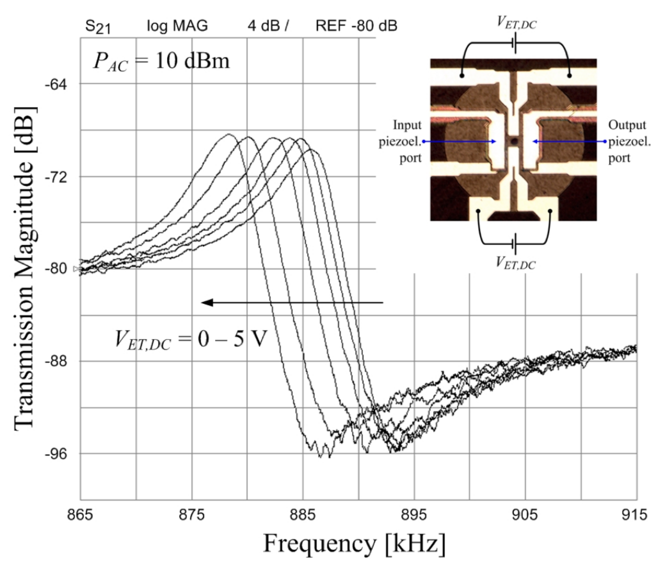

Fig. 3. Two-port measurements of the transmission frequency response for the piezoelectrically actuated device using the AC signal with 10 dBm power, and tuned with different DC voltages $V_{ET,DC}$ simultaneously applied to the both electrothermal tuning electrodes.

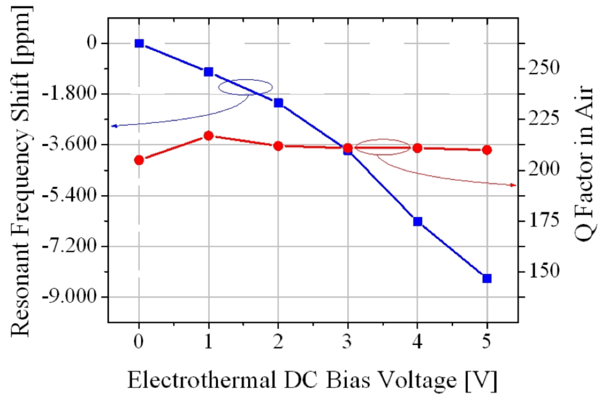

Fig. 4. Measured resonant frequency shift and Q factor in air of the piezoelectrically actuated device using the AC signal of 10 dBm power, and tuned with different DC voltages $V_{ET,DC}$ simultaneously applied to the both electrothermal tuning electrodes.

frequency shift of about -8,400 ppm (frequency tuning range of about 7.4 kHz) has been measured (Fig. 4). A wider tuning range would be achieved probably if the measurements, under the same actuation conditions, were performed in vacuum conditions [35], [36]. The decrease of the resonant frequency detected as the DC voltage increases is attributed to the change of stress in the diaphragm induced by the electrothermal heating [20], [37]. Fig. 4 also shows the Q factor in air as a function of the electrothermal DC tuning voltage. Vacuum measurements should provide significantly higher Q factor values [38]. The observed small variations of the Q factor in air (within 5 %) as the electrothermal DC tuning voltage increases, together with the almost constant transmission magnitudes (insertion losses) in Fig. 3, suggest that the device under the electrothermal frequency tuning operation still preserve steady bandwidth with limited influence of the motional impendence, which is very important for use in filtering and oscillator applications. The negligible variation of the insertion loss (Fig. 3) is consistent with previous findings with the electrostatically actuated and electrothermally tuned resonators [18].

B. Piezoelectric tuning

Piezoelectric transduction can be used for actuation but also for tuning the resonant frequency by applying DC bias voltage [9]. Fig. 5 shows the transmission magnitude plots of the device tuned piezoelectrically using the same DC bias voltages as in the case of the electrothermal tuning. The piezoelectric tuning has been performed by superimposing a DC signal provided by an external DC power supply on the actuating AC signal from the network analyzer. A constant input AC signal power of 10 dBm has been applied while DC voltage has been swept in the range of 0 V - 5 V with a step of 1 V. In these measurements, the electrodes reserved for electrothermal tuning have been grounded. With a DC voltage increase from 0 V to 5 V, the frequency tuning range of about 2.1 kHz has been obtained (frequency shift of about 2,400 ppm). The obtained frequency tuning range is about three

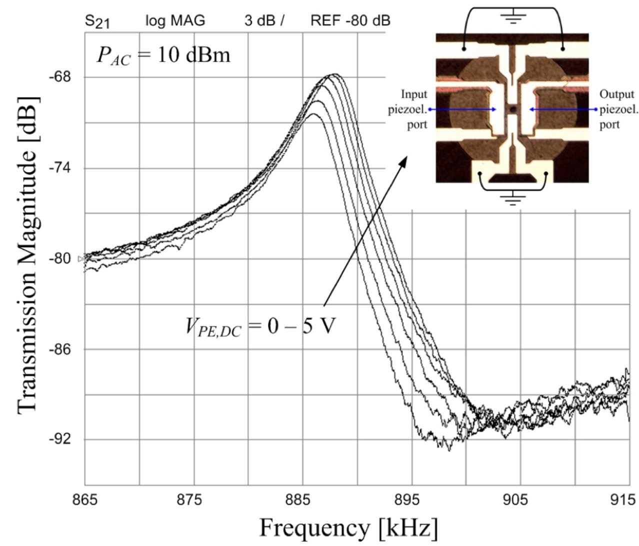

Fig. 5. Transmission magnitude plots of the device actuated by applying the the AC signal with 10 dBm power and different DC voltages $V_{PE,DC}$ to the input piezoelectric port. The electrothermal electrodes were grounded.

times narrower than the electrothermally tuning range. The increase in resonant frequency detected when increasing the DC voltage is attributed to the effect of the DC bias field on the stress of the piezoelectric layer (1) [26]. As the DC bias voltage increases, the stress within the structure induced by the piezoelectric layer increases thus influencing the resonant frequency of the device [10]. Unlike electrothermal tuning, piezoelectric tuning has shown a noticeable increase in transmission magnitude (decrease of the motional resistance) and a decrease of the Q factor in air, corresponding to our previous findings with piezoelectrically transduced double-clamped beam resonators [10], as well as other research groups [9], [39]-[42].

C. Stress Analysis

In order to gain a better understanding of the difference between the measured electrothermal and piezoelectric

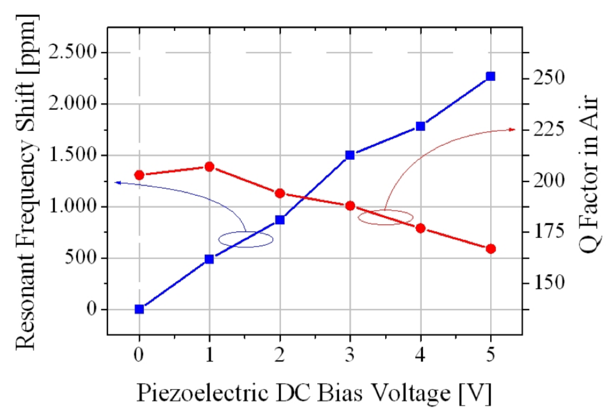

Fig. 6. Measured resonant frequency shift and Q factor in air of the piezoelectrically actuated device using the AC signal of 10 dBm power and different DC voltages $V_{PE,DC}$ to the input piezoelectric port. The electrothermal electrodes were grounded.

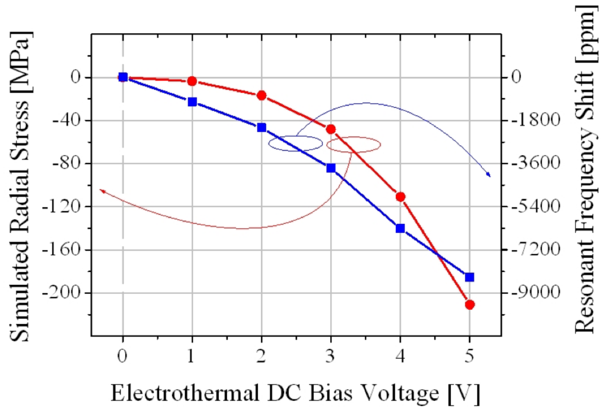

Fig. 7. Simulated electrothermally induced stress in 3C-SiC layer and measured resonant frequency shift versus tuning DC voltage.

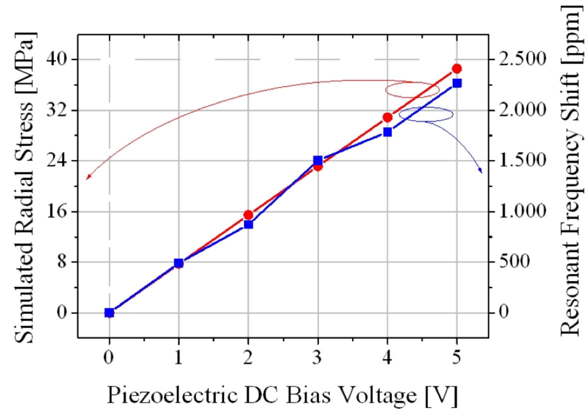

Fig. 8. Simulated piezoelectrically induced stress in 3C-SiC layer and measured resonant frequency shift versus tuning DC voltage.

frequency tuning range, a finite element model of the resonant device (including all the layers shown in Fig. 2) has been created using *CoventorWare*. Simulations have been performed to investigate the change in radial stress when the tuning voltages used in the experiments are applied to the structure. The radial stress is the stress in the direction between the center of diaphragm structure and the anchor and it has been extracted at the position below the input piezoelectric port (see Fig. 1).

First, a simulation has been performed to determine the value of built-in stress that should be assigned to the 3C-SiC layer. While the device is designed as a multilayer structure, only a small portion of the 3C-SiC diaphragm is covered with the piezoelectric ports and electrothermal electrodes (Fig. 1) and therefore, the influence of the residual stress of layers other than the 3C-SiC layer has been disregarded. It has been found that by including a tensile radial stress of 525 MPa, the simulated resonant frequency can be matched to the experimental value of 886 kHz for a 0 V DC tuning voltage. The model, now including the initial built-in stress, has been used to simulate the effect of electrothermally and piezoelectrically induced shifts in the radial stress.

Fig. 7 shows the change in simulated radial stress, together with the measured frequency shift previously given in Fig. 4, as a function of the electrothermal tuning DC voltage. The change in simulated induced radial stress of the piezoelectrically tuned device, together with the measured frequency shift previously given in Fig. 5, is shown on Fig. 8. The simulation results show clearly that the change of stress influences the resonant frequency of the device.

From Figs 7 and 8, it can be seen that electrothermal tuning reduces the radial stress, whereas piezoelectric tuning increases the radial stress, which corresponds to the decrease and increase in resonant frequency that has been measured. As the 3C-SiC diaphragm has a fairly large tensile residual stress, the simulation results indicate that electrothermal tuning mechanism effectively serves to reduce the tensile stress, relaxing the diaphragm. In addition, for a DC voltage increase from 0 V to 5 V, the resonant frequency shift has been simulated as -103,000 ppm for electrothermal tuning and +20,000 ppm for piezoelectric tuning, which is 12 times and 8 times, respectively, larger than the measured value, attributable to the lack of atmospheric damping in the FEM model. The observed frequency tuning range widening with atmospheric pressure reduction is consistent with previous experimental findings [35], [36].

In addition to the stress simulations, vertical displacements of the multilayer structure induced electrothermally (Fig. 9a) and piezoelectrically (Fig. 9b) by applying DC voltage of 1 V have been simulated. In the case of the electrothermally induced displacement, it can be seen that a temperature increase is induced throughout the structure, which leads to a deflection of the entire structure, as shown in Fig. 9a. However, the deflection induced piezoelectrically is seen only in the portion of the structure at the piezoelectric input port

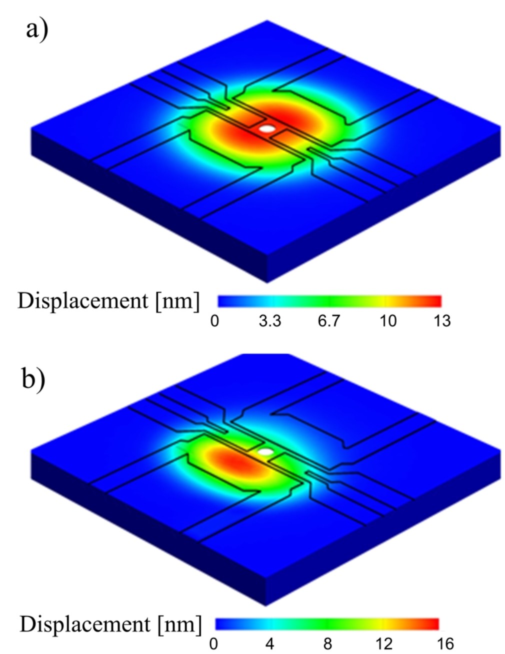

Fig. 9. Simulated vertical displacement of the multilayer structure induced (a) electrothermally and (b) piezoelectrically by applying DC voltage of 1 V.

(Fig. 9b). The observed simulation results indicate that localized nature of the piezoelectrically induced deflection affects the resonant frequency in a smaller manner compared to the electrothermal method, since only the piezoelectric input port has been used for tuning.

VI. Conclusions

A piezoelectrically transduced flexural-mode MEMS resonator that can be tuned electrothermally and piezoelectrically using DC voltages compatible with electronic circuits has been reported. The piezoelectric input and output ports composed of Pt/PZT/Pt together with electrothermal Pt electrodes are placed on the top of the 3C-SiC diaphragm with a central hole. The port and electrode designs are optimized to achieve high piezoelectric transduction efficiency and effective electrothermal tuning independently of the piezoelectric transduction. While the electrothermal tuning offers a downward frequency shift, the piezoelectrically induced tuning can be used to shift upward the untuned resonant frequency. The electrothermal tuning has been shown to be more efficient than the piezoelectric one, achieving more than three times wider frequency tuning range, with steady bandwidth and limited influence of the motional impendence, when applying equal DC voltages. FEM simulations have shown that a larger change in stress in the diaphragm is induced by an electrothermal tuning voltage, explaining the wider frequency tuning range compared to the piezoelectric case. In addition, the electrothermal tuning mechanism has been shown to lead to the relaxation of the tensile residual stress in the 3C-SiC diaphragm. The low voltage tunability, independency of the input/output operation, simple fabrication process, minimal effect on the piezoelectric sensitivity and the fundamental resonant frequency make the integration of the electrothermal tuning very attractive for implementation in most piezoelectric resonators.

Acknowledgment

B. Sviličić acknowledges financial support of the Croatian Science Foundation and the University of Rijeka (grant 13.07.1.4.01).

References

[1] T. M. van Beek and R. Puers, “A review of MEMS oscillators for frequency reference and timing applications,” *J. Micromech. Microeng.*, vol. 22, pp. 013001-35, Jan. 2012.

[2] C. T.-C. Nguyen, “MEMS Technology for Timing and Frequency Control,” *IEEE Trans. Ultrason. Ferroelectr. Freq. Control*, vol. 54, pp.251-270, Feb. 2007.

[3] C. T.-C. Nguyen, “A 3D-HARPSS Polysilicon Microhemispherical Shell Resonating Gyroscope: Design, Fabrication, and Characterization,” *IEEE Sens. Journal*, vol. 15, pp. 4974-4985, Sep. 2015.

[4] X. Zou, P. Thiruvenkatanathan, and A. A. Seshia, “A Seismic-Grade Resonant MEMS Accelerometer,” *J. Microelectromech. Syst.*, vol. 23, pp. 768-770, Aug. 2014.

[5] F. Khoshnoud, and C.W. de Silva, “Recent advances in MEMS sensor technology-mechanical applications,” *IEEE Instrum. Meas. Mag.*, vol. 15, pp. 14–24, 2012.

[6] W. M. Zhang, K. M. Hu, Z. K. Peng, and G. Meng, “Tunable Micro- and Nanomechanical Resonators,” *Sensors*, vol. 15, pp. 26478-26566, 2015.

[7] M. L. C. de Laat, H. H. Pérez Garza, J. L. Herder, and M. K. Ghatkesar, “A review on in situ stiffness adjustment methods in MEMS,” *J. Micromech. Microeng.*, vol. 26, pp. 063001-21, 2016.

[8] D.L. DeVoe, “Piezoelectric thin film micromechanical beam resonators,” *Sens. Actuators A*, vol. 88, pp. 263-272, Jan. 2001.

[9] H. Chandrahalim, S.A. Bhave, R. Polcawich, J. Pulskamp, D. Judy, R. Kaul, and M. Dubey, “Performance comparison of $Pb(Zr_{0.52}Ti_{0.48})O_3$-only and $Pb(Zr_{0.52}Ti_{0.48})O_3$-on-silicon resonators,” *Appl. Phys. Lett.*, vol. 93, pp. 233504-233504-3, 2008.

[10] B. Sviličić, E. Mastropaolo, T. Chen, and R. Cheung, “Piezoelectrically Transduced Silicon Carbide MEMS Double-Clamped Beam Resonators,” *J. Vac. Sci. Technol. B*, vol. 30, pp. 06FD05-1- 06FD05-7, Nov. 2012.

[11] G. Piazza, E. Abdolvand, G. K. Ho, and F. Ayazi, “Voltage-tunable piezoelectrically-transduced single-crystal silicon micromechanical resonators,” *Sens. Actuators A*, vol. 111, pp. 71-78, Mar. 2004.

[12] D. E. Serrano, R. Tabrizian, and F. Ayazi, “Electrostatically tunable piezoelectric-on- silicon micromechanical resonator for real-time clock,” *IEEE Trans. Ultrason., Ferroelectr., Freq. Control*, vol. 59, pp. 358-365, Mar. 2012.

[13] M. Y. Elsayed, P. V. Cicek, F. Nabki, and M. N. El-Gamal, “Bulk Mode Disk Resonator With Transverse Piezoelectric Actuation and Electrostatic Tuning,” *J. Microelectromech. Syst.*, vol. 25, pp. 252-261, Apr. 2016.

[14] A. Norouzpour-Shirazi, M. Hodjat-Shamami, R. Tabrizian, and F. Ayazi, “Dynamic Tuning of MEMS Resonators via Electromechanical Feedback,” *IEEE Trans. Ultrason., Ferroelectr., Freq. Control*, vol. 62, pp. 129-137, Jan. 2015.

[15] G. Hummel, Y. Hui, and M. Rinaldi, "Reconfigurable Piezoelectric MEMS Resonator Using Phase Change Material Programmable Vias", *J. Microelectromech. Syst.*, vol. 24, pp. 2145-2151, Dec. 2015.

[16] H. Göktas, and M. E. Zaghloul, “Tuning In-Plane Fixed–Fixed Beam Resonators With Embedded Heater in CMOS Technology,” *IEEE Electron Device Lett.*, vol. 36, pp. 189-191, Feb. 2015.

[17] W. Zhang, and J. E. Y. Lee, “Characterization and modeling of electro-thermal frequency tuning in a mechanical resonator with integral crossbar heaters,” *Sens. Actuators A*, vol. 202, pp. 69-74, 2013.

[18] F. Nabki, T. A. Dusatko, S.Vengallatore, and M. N. El-Gamal, “Low-Stress CMOS-Compatible Silicon Carbide Surface-Micromachining Technology—Part II: Beam Resonators for MEMS Above IC,” *J. Microelectromech. Syst.*, vol. 20, pp. 720-729, Jun. 2011.

[19] C. M. Jha, M. A. Hopcroft, S. A. Chandorkar, J. C. Salvia, M. Agarwal, R. N. Candler, R. Melamud, B. Kim, and T. W. Kenny, “Thermal Isolation of Encapsulated MEMS Resonators,” *J. Microelectromech. Syst.*, vol. 17, pp. 175-729, Feb. 2008.

[20] B. Sviličić, E. Mastropaolo, and R. Cheung, “Widely tunable MEMS ring resonator with electrothermal actuation and piezoelectric sensing for filtering applications,” *Sens. Actuators A*, vol. 226, pp. 149-153, May 2015.

[21] C.S. Jun, X.M.H. Huang, M. Manolidis, C.A. Zorman, M. Mehregany, and J. Hone, “Electrothermal tuning of Al-SiC nanomechanical resonators,” *Nanotechnology*, vol. 17, pp. 1506-1511, Feb. 2006.

[22] G. Zhang *et al.*, “Active frequency tuning for magnetically actuated and piezoresistively sensed MEMS resonators,” *IEEE Electron Device Lett.*, vol. 34, no. 7, pp. 921–923, Jul. 2013.

[23] B. Kim, R. H. Olsson, and K. E. Wojciechowski, “Ovenized and thermally tunable aluminum nitride microresonators,” in *Proc. IEEE Int. Ultrason. Symp.*, San Diego, CA, USA, Oct. 2010, pp. 974–978.

[24] A. Tazzoli, M. Rinaldi, and G. Piazza, “Experimental investigation of thermally induced nonlinearities in aluminum nitride contour-mode MEMS resonators,” *IEEE Electron Device Lett.*, vol. 33, no. 5, pp. 724–726, May 2012.

[25] B. Kim, J. Nguyen, K. E. Wojciechowski, and R. H. Olsson, "Oven-Based Thermally Tunable Aluminum Nitride Microresonators", *J. Microelectromech. Syst.*, vol. 22, pp. 265-275, Apr. 2013.

[26] Q.M. Wang, T. Zhang, Q. Chen, and X.H. Du, “Effect of DC bias field on the complex materials coefficients of piezoelectric resonators”, *Sens. Actuators A*, vol. 109, pp. 149-155, Dec. 2003.

[27] Y.T.Yang,K.L.Ekinci,X.M.H.Huang,L.M.Schiavone,M.L.Roukes, C. A. Zorman, and M. Mehregany, “Monocrystalline silicon carbide nano-electromechanical systems,” *Appl. Phys. Lett.*, vol. 78, pp. 162–164, Jan. 2001.

[28] V. Cimalla, J. Pezoldt, and O. Ambacher, “Group III nitride and SiC based MEMS and NEMS: Materials properties, technology and applications,” *J. Phys. D, Appl. Phys.*, vol. 40, pp. 6386–6434, 2007.

[29] P. M. Sarro, “Silicon carbide as a new MEMS technology,” *Sens. Actuators A*, vol. 82, pp. 210–218, May 2000.
[30] B. Sviličić, E. Mastropaolo, and R. Cheung, “Piezoelectric sensing of electrothermally actuated silicon carbide MEMS resonators,” *Microelectronic Eng.*, vol. 119, pp. 24-27, Sep. 2014.
[31] J. Lu, T. Ikehara, Y. Zhang, T. Mihara, T. Itoh, and R. Maeda, “High Quality Factor Silicon Cantilever Transduced by Piezoelectric Lead Zirconate Titanate Film for Mass Sensing Applications,” *Jpn. J. Appl. Phys.*, vol. 46, pp. 7643–7647, 2007.
[32] P. Srinivasan and M. Spearing, "Effect of heat transfer on materials selection for bimaterial electrothermal actuators", *J. Microelectromech. Syst.*, vol. 17, pp. 653-667, Mar. 2008.
[33] E. Mastropaolo and R. Cheung, “Electrothermal actuation of silicon carbide ring resonators,” *J. Vac. Sci. Technol. B*, vol. 27, pp. 3109-3114, Nov. 2009.
[34] E. Mastropaolo, B. Sviličić, T. Chen, B. Flynn, and R. Cheung, “Piezo-electrically actuated and sensed silicon carbide ring resonators,” *Microelectronic Eng.*, vol. 97, pp. 220-222, Sep. 2012.
[35] A. Rahafrooz, A. Hajjam, B. Tousifar, S. Pourkamali, Thermal actuation, a suitable mechanism for high frequency electromechanical resonators, in *IEEE Int. Conf. on Micro Electro Mechanical Systems*, pp. 200-203, 2010.
[36] H. J. Hall, A.Rahafrooz, J. J. Brown, V. M. Bright, S. Pourkamali, Thermally actuated I-shaped electromechanical VHF resonators, in *IEEE Int. Conf. on Micro Electro Mechanical Systems*, pp. 737–740, 2012.
[37] B. Sviličić, E. Mastropaolo, B. Flynn, and R. Cheung, “Electrothermally Actuated and Piezoelectrically Sensed Silicon Carbide Tunable MEMS Resonator,” *IEEE Electron Device Lett.*, vol. 33, pp. 278-280, Feb. 2012.
[38] F. R. Blom, S. Bouwstra, M. Elwenspoek, and J. H. J. Fluitman, “Dependence of the quality factor of micro-machined silicon beam resonators on pressure and geometry,” *J. Vac. Sci. Technol. B, Microelectron. Nanometer Struct.*, vol. 10, pp. 19–26, Jan./Feb. 1992.
[39] J. Conde, and P. Muralt, “Characterization of Sol-Gel $Pb(Zr_{0.53}Ti_{0.47})O_3$ in Thin Film Bulk Acoustic Resonators,” *IEEE Trans. Ultrason., Ferroelectr., Freq. Control*, vol. 55, pp. 1373-1379, Jun. 2008.
[40] S. S. Bedair, D. Judy, J. Pulskamp, R. G. Polcawich, A. Gillon, E. Hwang, S. Bhave, “High rejection, tunable parallel resonance in micromachined lead zirconate titanate on silicon resonators,” *Appl. Phys. Lett.*, vol. 99, pp. 103509-1-103509-3, 2011.
[41] J. S. Pulskamp, R. Q. Rudy, S. S. Bedair, J. M. Puder, M. G. Breen, R. G. Polcawich, Ferroelectric PZT MEMS HF/VHF resonators/filters, in *IEEE Int. Freq. Control Symp.*, pp. 1-4, 2016.
[42] R. Q. Rudy, J. S. Pulskamp, S. S. Bedair, J. M. Puder, and R. G. Polcawich, Piezoelectric disk flexure resonator with 1 dB loss, in *IEEE Int. Freq. Control Symp.*, pp. 1-4, 2016.

Boris Sviličić received the diploma in electrical engineering (5 year curricula) from the Faculty of Electrical Engineering and Computing, University of Zagreb, in 1999. Master of science and doctorate of science degrees in electronics engineering he received from the same institution in 2003 and 2008 respectively. He is currently a full professor with the Faculty of Maritime Studies, University of Rijeka. His research interests involve design, simulation, fabrication and characterization of MEMS based sensors and actuators, and analytical modeling and simulation of novel CMOS devices based on silicon-on-insulator technology.

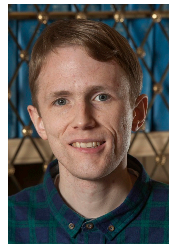

Graham S. Wood (M’10) received the M.Eng degree in electronics and electrical engineering and the M.Sc. degree in microelectronics from the University of Edinburgh, Edinburgh, U.K., in 2008 and 2011, respectively, and the Ph.D. degree in microelectromechanical systems from the University of Southampton, Southampton, U.K., in 2016. He is currently a Research Associate with the Scottish Microelectronics Centre, Institute for Integrated Micro and Nano Systems, School of Engineering, University of Edinburgh. He held the same position from 2008 to 2010, where he conducted research concerning the actuation and sensing of SiC MEMS resonators for high frequency RF applications. His current research involves the use of graphene resonating structures as acoustic transducers.

Enrico Mastropaolo (M’14) received the Laurea degree in micro-electronics engineering from the Univeristà degli Studi di Padova, Italy, in 2006, and the Ph.D. degree in microsystems and microfabrication from the University of Edinburgh, UK, in 2011. He is currently a lecturer with the Scottish Microelectronics Centre, Institute for Integrated Micro and Nano Systems, in the School of Engineering of the University of Edinburgh. His research interests include design, simulation, fabrication and characterization of microelectromechanical systems (MEMS) and transduction techniques for microsystems. His current research work on MEMS focusses on SiC and graphene as structural materials, biomimetic design, and embedment of polymer nanocomposites and nanostructures in microsystems.

Professor Rebecca Cheung FRSE (M’96, SM’02) received first class honours and Ph.D degrees in Electronics and Electrical Engineering from the University of Glasgow, U.K., in 1986 and 1990, respectively. She currently holds a Chair in Nanoelectronics in the School of Engineering at the University of Edinburgh, U.K. Professor Cheung has an international reputation for her contribution in the development and application of micro- and nano-fabrication. More recently, her research focusses on microresonators and microelectromechanical systems. She has published over 200 scientific articles, 1 patent and 1 book in related topics.